Solar Facilities for the European Research Area

SFERA-III

Solar Facilities for the European Research Area

D10.5: "Report about increased robustness of the CYI Fresnel research infrastructure against DNI variation"

Estimated delivery date:	31/12/2022
Actual delivery date:	21.10.2019
Lead beneficiary:	The Cyprus Institute (CyI)
Person responsible:	Alaric Christian Montenon
Deliverable type:	☒ R ☐ DEM ☐ DEC ☐ OTHER ☐ ETHICS ☐ ORDP
Dissemination level:	☒ PU ☐ CO ☐ EU-RES ☐ EU-CON ☐ EU-SEC

THIS PROJECT HAS RECEIVED FUNDING FROM THE EUROPEAN UNION'S HORIZON 2020 RESEARCH AND INNOVATION PROGRAMME UNDER GRANT AGREEMENT NO **823802**

AUTHORS

Author	Institution	E-mail
Alaric Christian Montenon	CyI	a.montenon@cyi.ac.cy
Diogo Canavarro	UEVORA	diogocvr@uevora.pt
Patrícia Scalco	UEVORA	ex16935@alunos.uevora.pt
João Marchã	UEVORA	joaomarcha@uevora.pt
Tiago Eusébio	UEVORA	tre@uevora.pt
André Santos	UEVORA	avas@uevora.pt

DOCUMENT HISTORY

Version	Date	Change
01	12/12/2022	

VALIDATION

Reviewers		Validation date
Marc Roeger	DLR	14/12/2022

DISTRIBUTION LIST

Date	Recipients
14.12.2022	WP10 Partners

Disclaimer

Executive Summary

The present deliverable deals is a complementary report following the D10.4. While in D10.4, the Cyprus Institute developed the *RealTrackEff* modelling to predict with an accuracy of less than 1°C of the outlet of the of its LFR, the present report deals with the control strategies applied to the collector in regards to DNI variations. The work carried out is linked to subtask 10.2.C and was also the scope of publication that is added as an annex file. The summary summarises the results at the Cyprus Institute in the first part and in the second part, the results of the LFR at U-EVORA are detailed.

1. The Linear Fresnel collector at the Cyprus Institute

Within D10.4 (Report on accuracy of transient linear Fresnel collector testing). Franhofer and the Cyprus Institute worked together to compare their respective methodologies to determine the quasi dynamic behaviour of the Linear Fresnel Reflector at the Cyprus Institute [1]. This was the scope of a common publication following an oral presentation at SolarPaces conference 2020 [2]. The methodoly from the Cyprus Institute was called '*RealTrackEff*' and demostrated an accuracy of 1°C of RMSE (Root Mean Square Error) on 60 days of experimental data on about 100,000 sampled timesteps that encompasse measurements of flow rate, DNI, inlet temperature, outlet temperature and ambient temperature. IAMs had been priorly calculated on Tonatiuh++ software, currently under development at the Cyprus Institute.

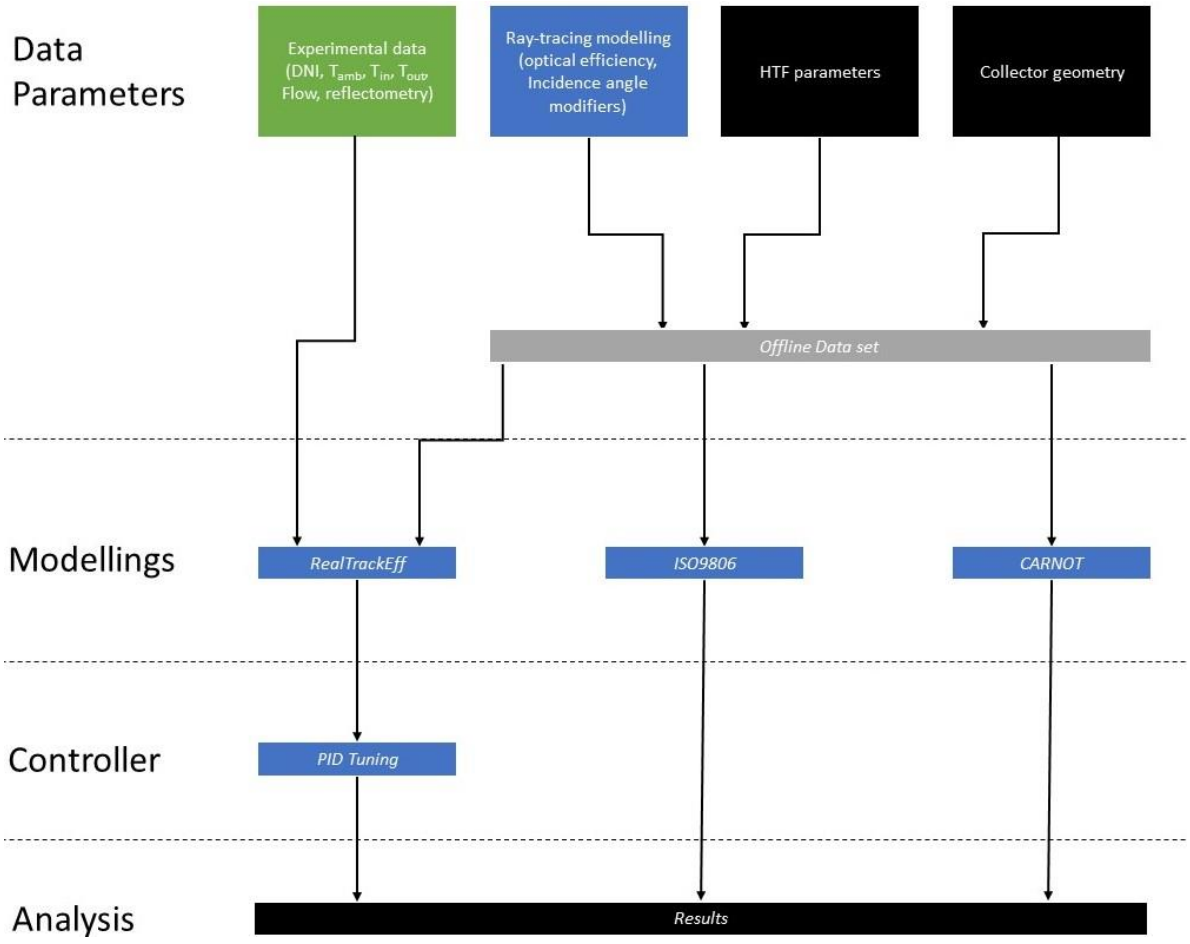

Figure 1: Flowchart of the methodology.

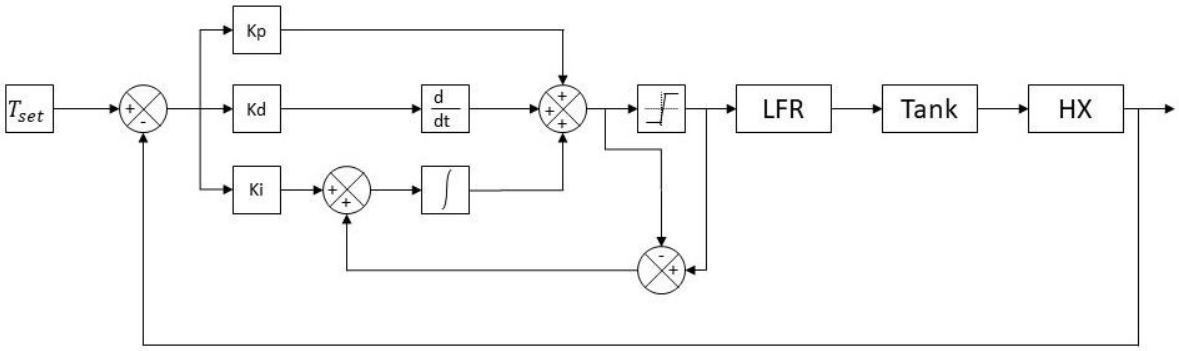

Figure 2: PID on the HTF loop with anti-windup.

The *RealTrackEff* demostrated its capacity in rendering asymmetric behaviour. It has been implemented in Matlab/Simulink and optimum PID control has been calculated based on it. The related work has been released as a substantial part of a scientific paper in collaboration with the Helwan University, Cairo, Egypt who uses the *CARNOT* modelling [3]. As a matter of comparison the reference *ISO 9806* modelling has also be used [4] as this is the reference standard for solar thermal collectors. It has been demonstrated to be weaker in terms of accuracy in D10.4. The PID has been tuned in order to reach a stable operation of the HTF (Heat Transfer Fluid) at the outlet of the receiver. The principles of the development are presented in Figure 1 and the PID architecture, in Figure 2. The whole heat transfer fluid loop has been modelled including the adiabatic buffer of oil (Tank), thus inertia, and the heat-exchange with the user side.

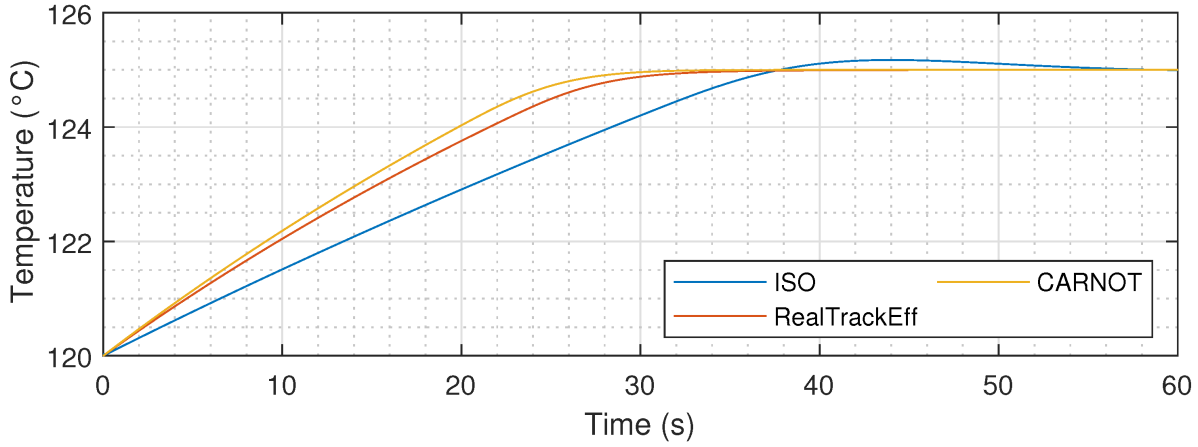

Figure 3: Temperature of the HTF at the outlet of the LFR, response to a step of 125°C starting at 120°C at time 0s.

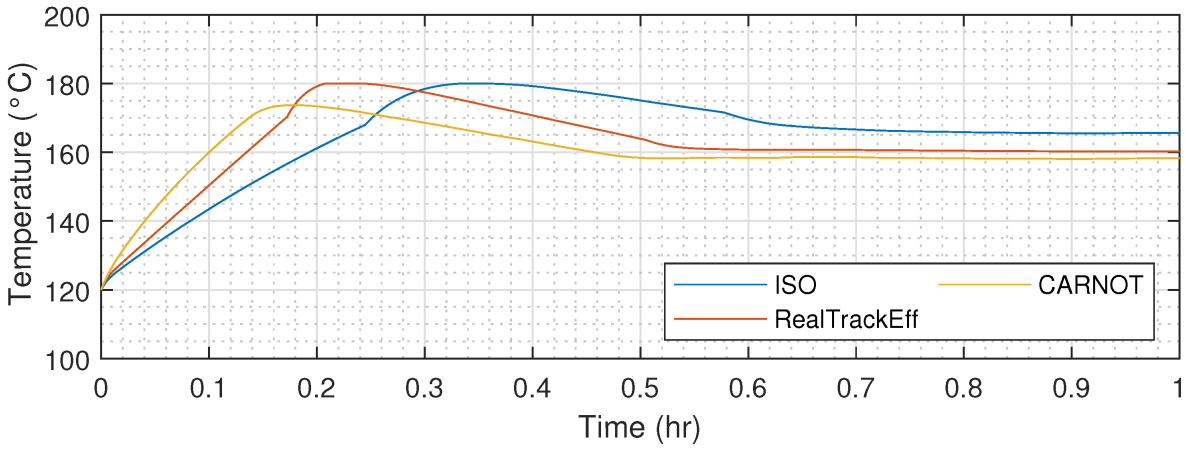

Figure 4: Oil buffer average tempertaure with a reference of 160°C with an initial temperature of 120°C on the absorber

First, to tune the PID, a step in reference of the outlet temperature had been applied to the HTF from 120°C to 125°C, on the LFR's model only (Figure 3). The PID tuning demonstrated a good accuracy in the reference tracking compared to the ISO9806 model, as it offers faster response (32s vs 54s) without any overshooting (+ 4% in the ISO). As a second step the PID was tested on the whole loop as presented in Figure 2. For instance the average tank temperature (oil buffer) is displayed on Figure 4. As can be seen, it reaches 0.2°C against variable DNI and ambient temperature while the ISO has a permanent state of 5.6°C. The stabilisation occurs faster as well: 35 min minutes against 45 minutes. This leads to an impact on the energy performance predictions as shown in Figure 5. Indeed while the *ISO 9806* predicts a power output of 42 kW while the *RealTrackEff* predicts 26 kW. Thus, this leads to an overestimation of 61%. Eventually the study demonstrated the importance of the modelling accuracy as it has direct consequences on the annual performance of LFRs.

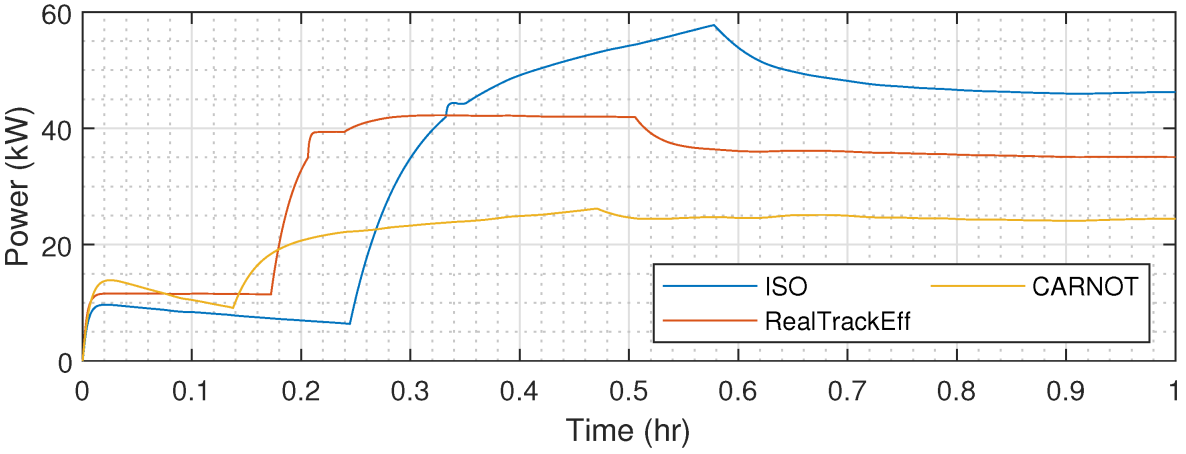

Figure 5: Power output prediction of the modelling with tuned PID.

2. The linear Fresnel collector at the University of Evora

In this section, are presented and discussed the results obtained experimentally through tests on the linear collector at the University of Évora (UEVORA), the ALFR – Advanced Linear Fresnel Reflector (see Figure 6). The ALFR collector is a novel concept developed by the Renewable Energies Chair of UEVORA [4] targeting an optimized operation with Molten Salts up to 565ºC as Heat Transfer Fluid. Apart from the activities carried out in SFERA-III, the concept development and implementation has been supported by ALFR-Alentejo [5] and INIESC ÉVORA CONNECT [6] projects.

The ALFR collector has 19 heliostats with 0.32 m of width and 4 m of length (total primary area of 24.32m^2), with an estimated thermal peak power of around 16kW$_{th}$. It has an evacuated tubular receiver positioned at 4.57 m of height (Schott PTR70) surrounded by an optimized asymmetric Compound Elliptical Concentrator (CEC) secondary mirror to increase the overall concentration factor (around 28X). The thermal fluid used is the Fragoltherm® X-75-A.

Figure 6: The ALFR prototype collector.

The collector tests were performed in an azimuthal tracking platform (PECS – Solar Concentrators Testing Platform – an infrastructure part of SFERA-III's services network), whose characteristics are given by the Table 1.

Table 1. Testing platform characteristics.

Width	13 m	**Length**	18 m
Azimuth range	-120°, +120°	**Tilt range**	0°, 40°
Azimuth track. Accep.	≤ 0.5°	**Elev. Track. accur.**	≤ 0.5°
Maximum load	7100 kg	**Max. oper. Wind speed**	12 m/s

Figure 7 shows the experimental aparatus with the platform tilted on a N-S mounting orientation to reach normal incidence at solar noon. These were the first tests carried out but as shall be discussed next a E-W mounting orientation was eventually selected due to practical constrains.

Figure 7: The experimental test of the ALFR collector using the PECS platform.

The tests were carried out on September 26th, 27th, and 28th – at solar noon, and at ambient temperature (to exclude thermal losses terms of the useful power estimation, enabling only optical effects assessment) – with the collector positioned with an east-west mounting, having a tilt angle of β = 0° (horizontal plane), guaranteeing that the collector azimuth was the same of solar azimuth, for the duration of the tests through the rotation of PECS platform. The collector orientation is justified by the fact that the tests were carried out after the equinox (out of the range of the platform maximum tilt – 40°), and in addition, the results for the north-south orientation were compromised due to mechanical problems in the prototype related to tilting mounting position. The control parameters of the operation follow the requirements of ISO 9806:2017. The test conditions and mean values are shown in Table 2.

Table 2. Conditions and mean values.

Parameters	Maximum Value	Minimum Value	Average Value	Maximum Deviation
Mass Flow (kg/h)	8504.12	8497.33	8499.97	3.39 (0.03 %)
DNI (W/m²)	935.76	901.27	926.75	17.24 (1.86 %)
Amb. Temp. (°C)	25.35	20.39	23.46	2.47 (10.55 %)
Inlet Temp. (°C)	23.49	23.42	23.46	0.03 (0.13 %)

It is important to highlight that the values of temperature did not vary more than 1°C, and the mass flow was kept stable within 1% of fluctuation throughout the tests. Figure 8 shows that the temperatures and mass flow meet the ISO 9806:2017 test parameters. Figure 8 shows that the temperatures and mass flow meet the ISO 9806:2017 test parameters.

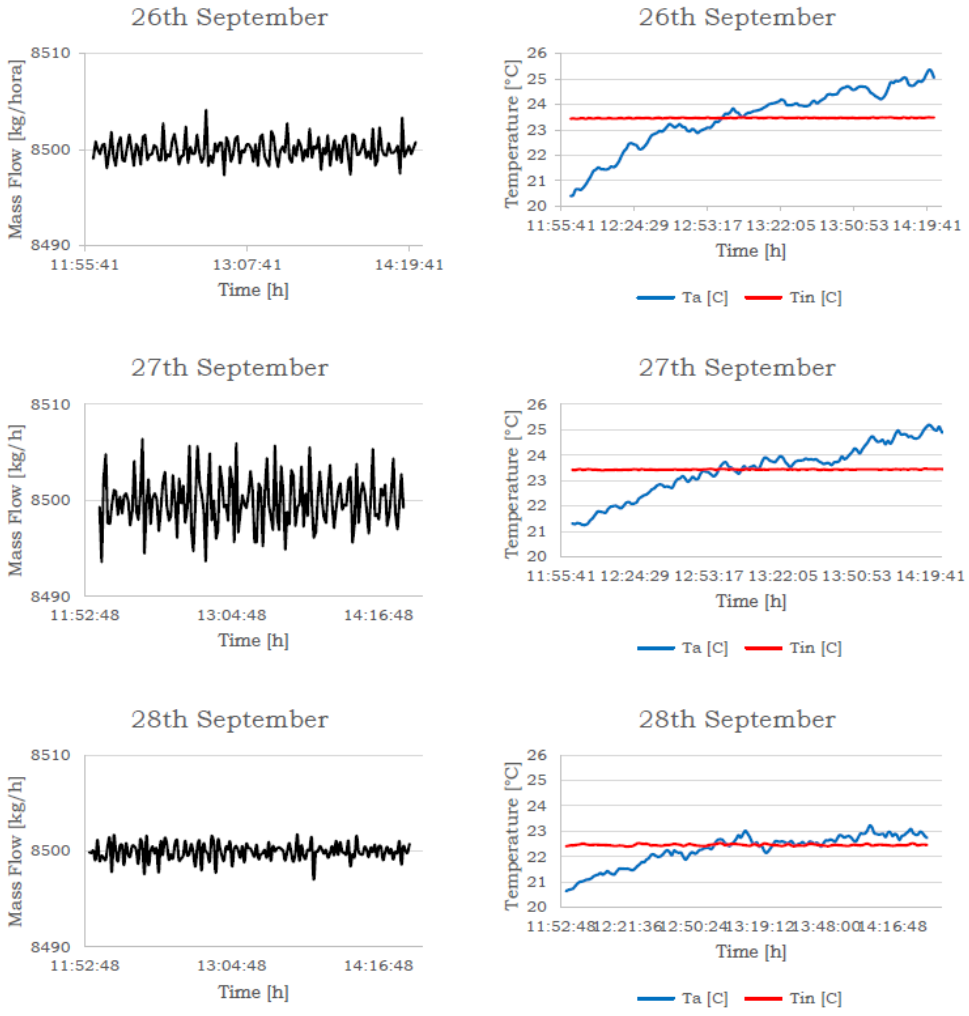

Figure 8: Mass Flow and Temperatures conditions for three-days tests: 26th, 27th, and 28th September.

(a) 26th September

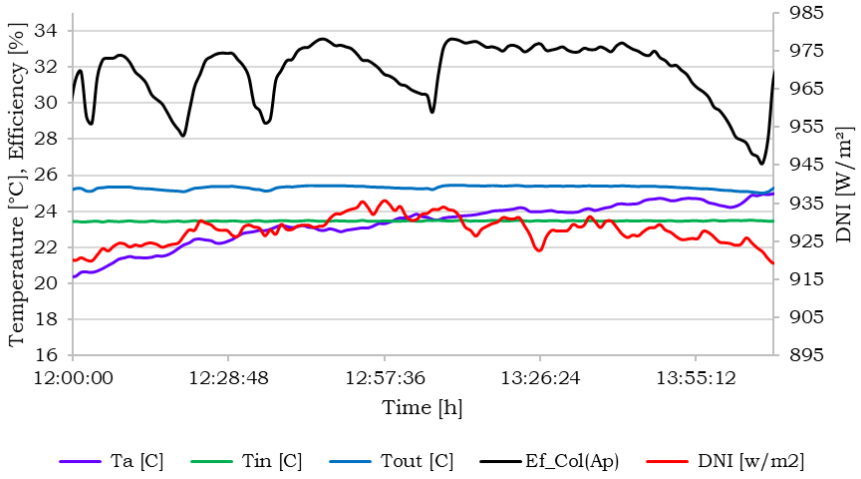

(b) 27th September

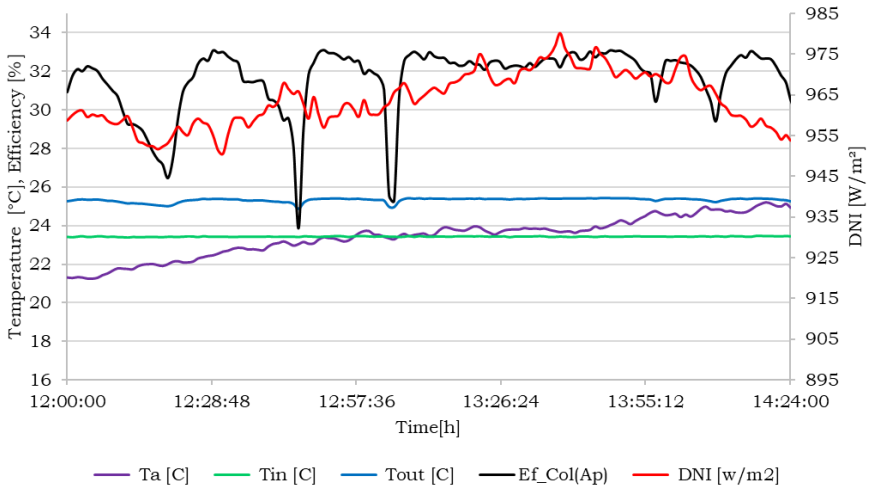

(c) 28th September

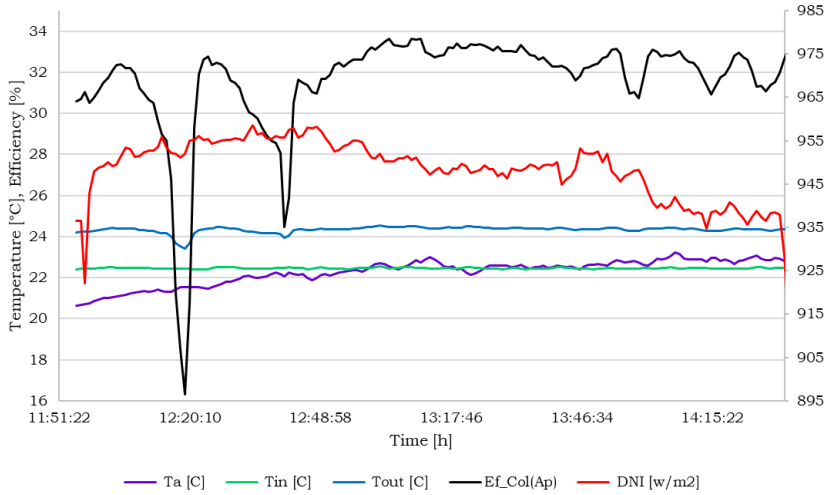

Figure 9: Representation of collector efficiency, Direct Normal Irradiance, and inlet, outlet, and ambient temperatures as a function of time for the three-days tests: (a) 26th September, (b) 27th September, and (c) 28th September.

Figure 9 presents the collector efficiency, Direct Normal Irradiance, and inlet, outlet, and ambient temperatures as a function of time for the three-days tests. The efficiency oscillation under stable solar irradiation, inlet temperature, and mass flow conditions is mainly due to prototype primary mirrors tracking problems.

To mitigate this problem, manual adjustments on mirror's position were carried out during the tests. These adjustments although not advisable were a practical attempt to characterize the performance of the prototype, by maintaining the stable solar flux on the receiver as much as possible. In fact, as shown in Figure 9 related to last day (28th of September) of test the oscillations were smaller from 12h30m, that is, the tracking problem was eventually minimized.

Since the tests were carried out without normal incidence (the collector is on an east-west mounting and horizontal plane) a correction factor of the useful primary area is required (cosine losses – see Table 3). The efficiency was calculated using the relation between the DNI and the area of the collector (see Equation 1).

$$\eta = \frac{P_{col}}{P} = \frac{P_{col}}{D\ NI.A.F_{cosine}} \qquad (1)$$

Table 3. Solar noon and solar height for the definition of the cosine effect coefficient.

Date	Solar noon [h]	Max. solar height [°]	Min. solar height [°]	Avg. solar height [°]	Cos Effect [-]*
26/09	13:23:03	50.11	44.5	47.3	0.68
27/09	13:22:43	49.73	44.5	47.1	0.68
28/09	13:22:23	49.34	44.5	46.9	0.68

* The considered cosine effect is measured between the plane of the primary mirrors, and the angle from normal to solar angles.

Figure 10 shows the efficiency results for the three-day testing. The obtained efficiency values were in the range of 53 %. This value is lower than the expected peak efficiency near 70 % [1] (considering a ray tracing calculation carried out before the campaign [4]). In fact, the effective efficiency is dependent on cosine effect, reflectivity, shading, tracking, geometric errors, mirror cleaning, and other losses. These loss values were not experimentally quantified in this campaign to compare with simulation calculation, as their assessment is demanding and the campaign was

[1] Note: This 70% value was considering a normal incidence, a situation that in practice was not possible to achieve due to the limitation concerning the N-S mounting. Nevertheless, this was still considered here as the reference value.

focused on the operation of the collector. However, typical values for these coefficients are presented in Table 4 [7].

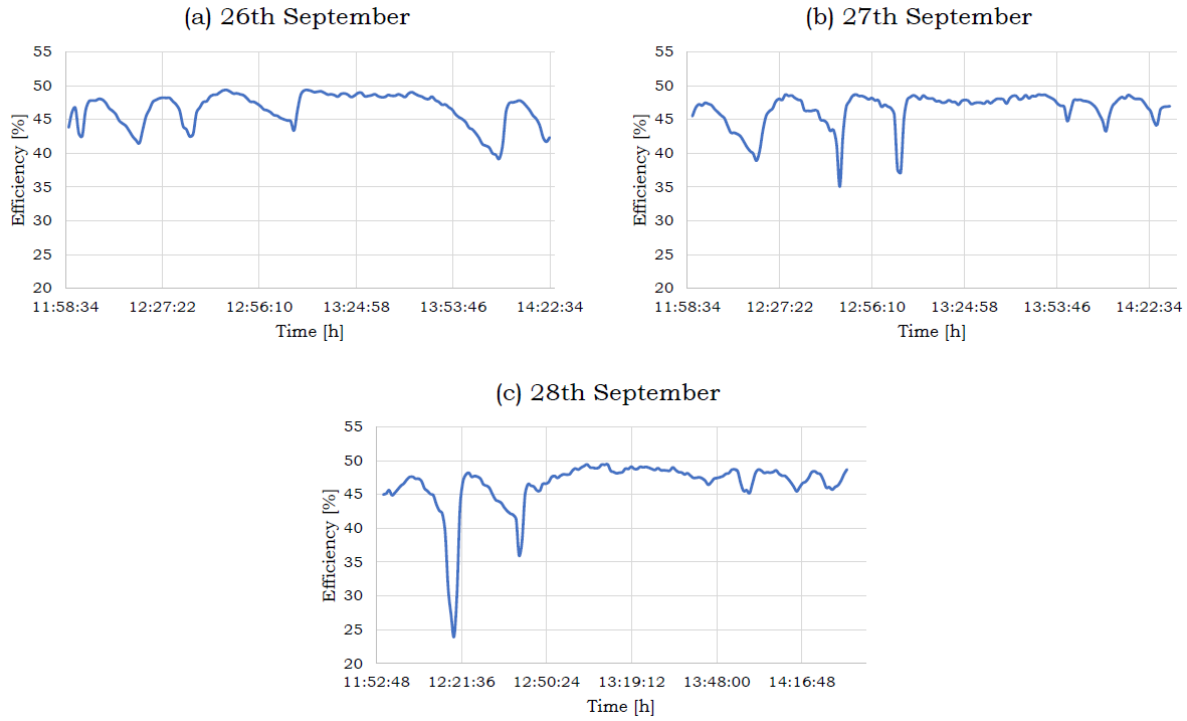

Figure 10. Corrected efficiency values for the three-days tests: (a) 26th September, (b) 27th September, and (c) 28th September.

Figure 11 shows that there is a clear mechanical and/or tracking problem with the mirrors (highlighted in red), since the sunlight is not clearly focused on the target (reducing the intercept factor). Therefore, it was concluded that tracking and geometric errors might be more severe than the presented values in Table 4, leading to lower to a lower efficiency than the reference value.

Table 4. Theoretical coefficients associated with losses in LFR concentrator, adapted from Forristal [7].

Associated Error	**Value [-]**
Reflectivity	0.92
Shading	0.974
Tracking	0.994
Geometric error	0.980
Mirror cleaning	1
Other losses	0.960

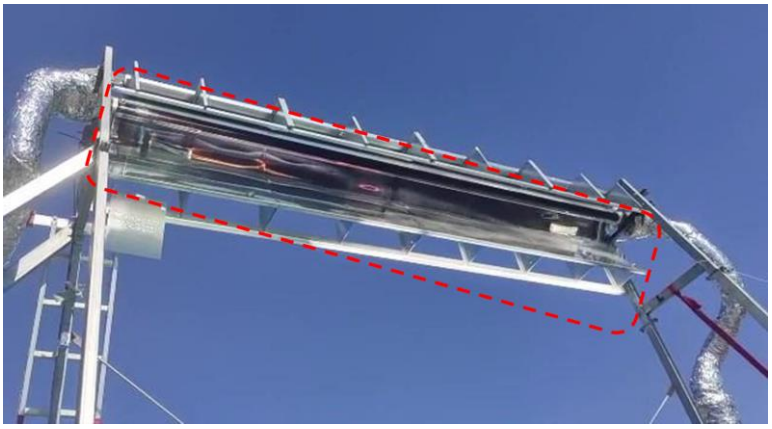

Figure 11. Tracking and geometrical issue in focusing the sun lighting on the target.

As a result of this campaign the following conclusions were taken:

1) The experimental operation was successful as the tests fulfilled the requirements of ISO 9806:2017. Additionally, PECS platform capabilities to tilt such systems safely were proven.

2) The efficiency of the collector was lower than expected. This could be justified by two major factors:

    a. ALFR collector is a prototype that has never been tested before and, therefore, a learning-curve process is required to understand better its behaviour.
    b. The structure of the collector might not have been sufficient to withstand with tilting at PECS, as the collector is meant to be placed horizontally on the ground. This might lead to important structural defects which has impact on the experimental result.

3) Structural and tracking improvements are required as next steps to consolidate the performance of the collector.

4) New tests are required to understand the full potential of the collector, particularly the performance of the secondary optics.

As a final comment, it is important to stress that such experimental campaigns are a key-point for the development of LFR technologies and attract the interest of industry on these solutions. As a matter of fact, a Portuguese company is already interested in this technology and a new LFR prototype will be tested at PECS with the collaboration of UEVORA.

3. References

[1] Alaric C. Montenon, Nestor Fylaktos, Fabio Montagnino, Filippo Paredes, and Costas N. Papanicolas, "Concentrated solar power in the built environment", AIP Conference Proceedings 1850, 040006 (2017) https://doi.org/10.1063/1.4984402

[2] Peter Schöttl, Alaric C. Montenon, Costas Papanicolas, Stephen Perry, and Anna Heimsath, "Comparison of advanced parameter identification methods for linear Fresnel collectors in application to measurement data", AIP Conference Proceedings 2445, 070012 (2022) https://doi.org/10.1063/5.0085892

[3] Montenon, A.C.; Meligy, R. Control Strategies Applied to a Heat Transfer Loop of a Linear Fresnel Collector. Energies 2022, 15, 3338. https://doi.org/10.3390/en15093338

[4] D. Canavarro, J. Chaves, M. Collares-Pereira, New Dual Asymmetric CEC Linear Fresnel Concentrator for Evacuated Tubular Receivers, in: AIP Conference Proceedings, 2017: p. 040001. doi:10.1063/1.4984397.

[5] ALFR-Alentejo Project (ALT20 03 0145 FEDER 039487). www.alfr-alentejo.uevora.pt

[6] INIESC ÉVORA-CONNECT Project (5114 ALT20 45 2020 67).

[7] Forristal, R. Heat Transfer Analysis and Modelling of a Parabolic Trough Solar Receiver Implemented in Engineering Equation Solver. Golden: National Renewable Energy Laboratory Technical Report, 2003.